1 **Light adaptation characteristics of melanopsin**
2
3
4
5 **Mukund Pant, [a, b] Andrew J. Zele, [a, b] Beatrix Feigl, [a, c, d] Prakash Adhikari [a, b, *]**
6
7
8
9 [a] *Centre for Vision and Eye Research, Queensland University of Technology (QUT), Brisbane,*
10 *QLD 4059, Australia*
11 [b] *School of Optometry and Vision Science, Queensland University of Technology (QUT),*
12 *Brisbane, QLD 4059, Australia*
13 [c] *School of Biomedical Sciences, Queensland University of Technology (QUT), Brisbane, QLD*
14 *4059, Australia*
15 [d] *Queensland Eye Institute, Brisbane, Australia*
16
17 *Corresponding author at: Visual Science and Medical Retina Laboratories, Centre for Vision
18 and Eye Research, QUT. 60 Musk Avenue, Kelvin Grove, Queensland 4059, Australia
19 E-mail address: p.adhikari@qut.edu.au (Prakash Adhikari)

20   **Abstract**

21   Following photopigment bleaching, the rhodopsin and cone-opsins show a characteristic
22   exponential regeneration in the dark with a photocycle dependent on the retinal pigment
23   epithelium. Melanopsin pigment regeneration in animal models requires different pathways to
24   rods and cones. To quantify melanopsin-mediated light adaptation, we first estimated its
25   photopigment regeneration kinetics through the photo-bleach recovery of the intrinsic
26   melanopsin pupil light response (PLR). An intense broadband light (~120,000 Td) bleached
27   43% of melanopsin compared to 86% of the cone-opsins. Recovery from a 43% bleach was
28   3.4X faster for the cone-opsin than melanopsin. Post-bleach melanopsin regeneration followed
29   an exponential growth with a 2.5 min time-constant (τ) that required 11.2 min for complete
30   recovery; the half-bleaching level (I_p) was ~4.47 log melanopic Td (16.10 log melanopsin
31   effective photons.cm^{-2}.s^{-1}; 8.25 log photoisomerisations.photoreceptor^{-1}.s^{-1}). The effect on the
32   cone-directed PLR of the level of the melanopsin excitation during continuous light adaptation
33   was then determined. We observed that cone-directed pupil constriction amplitudes increased
34   by ~10% when adapting lights had a higher melanopic excitation but the same mean
35   photometric luminance. Our findings suggest that melanopsin light adaptation enhances cone
36   signalling along the non-visual retina-brain axis. Parameters τ and I_p will allow estimation of
37   the level of melanopsin bleaching in any light units; the data have implications for quantifying
38   the relative contributions of putative melanopsin pathways to regulate the photopigment
39   bleach.

40

41   *Keywords:* Dark adaptation, Light adaptation, Melanopsin, Photopigment bleaching,
42   Photopigment regeneration, Pupil light response

1. Introduction

Following exposure to an intense light, the dark adaptation properties of the rod and cone pathways show a characteristic exponential recovery to their maximal sensitivity when quantified using visual psychophysics (Hollins & Alpern, 1973; Lamb & Pugh, 2004; Pianta & Kalloniatis, 2000; Wald et al., 1950), the electroretinogram (ERG) (Mahroo & Lamb, 2012; Paupoo et al., 2000; Thomas & Lamb, 1999), the pupil light response (PLR) (Alpern & Campbell, 1963; Alpern et al., 1959; Ohba & Alpern, 1972), and retinal densitometry (Alpern & Ohba, 1972). The regeneration time-constant is ~5X faster for the cone than rod pathways (Hecht et al., 1937; Lamb, 1981; Reuter, 2011). The dark adaptation photocycle is well-defined for rhodopsin and cone-opsins and requires the retinal pigment epithelium (RPE) to convert the all-trans retinal to 11-cis retinal (for review, Lamb & Pugh (2004)). Emerging evidence from mouse models of melanopsin photopigment regeneration indicates that it requires different pathways to rods and cones. Melanopsin might resist photic bleaching (Sexton et al., 2012) due to partial (Zhao et al., 2016) or complete independence (Tu et al., 2006) from the RPE for its photocycle and other characteristics including strong binding between its chromophore and opsin, conversion to an active meta-state following phototransduction (Sexton et al., 2012), and bistability (Mure et al., 2009) or tristability (Emanuel & Do, 2015). In humans, melanopsin-expressing intrinsically photosensitive retinal ganglion cells (ipRGCs) contribute to non-image forming control of the PLR (Adhikari et al., 2015; Cao et al., 2015; Gamlin et al., 2007; Gooley et al., 2012; Kardon et al., 2009; Markwell et al., 2010; Spitschan, 2019b; Tsujimura et al., 2010; Zele et al., 2019a) and circadian photoentrainment (Markwell et al., 2010; Provencio et al., 2000; Zele et al., 2011), and to image forming vision (Allen et al., 2019; Brown et al., 2012; Cao et al., 2015; DeLawyer et al., 2020; Spitschan, 2019a; Spitschan et al., 2017; Zele et al., 2019b; Zele et al., 2020b; Zele et al., 2018). To understand how melanopsin adapts to the light environment for regulating these phenomena, here we estimate melanopsin bleach and regeneration kinetics by measuring the melanopsin-directed PLR post-exposure to an intense light. Given that melanopsin-directed visual responses (Zele et al., 2019b; Zele et al., 2020b) and non-visual pupil responses (Adhikari et al., 2015; Gamlin et al., 2007) are first evident in high mesopic to low photopic illumination (20 – 200 Td), we measured melanopsin post-bleach recovery to a steady-state light adaptation level.

Light and dark adaptation optimise the visual response to environmental illumination level (Barlow, 1972) through adjustments of the sensitivity of rod and cone pathways (Barlow, 1972; Boff et al., 1986; Hecht et al., 1937; Hood & Finkelstein, 1986; Hood, 1998; Joselevitch, 2008; Lamb & Pugh, 2004; MacLeod, 1978; Zele & Cao, 2015). There is evidence from rodent models that melanopsin cells form independent postreceptoral pathways and receive extrinsic rod and cone inputs (Belenky et al., 2003; Güler et al., 2008) and also in non-human primates (Dacey et al., 2005). Also, melanopsin activation influences cone-mediated ERG in mice (Allen et al., 2014; Prigge et al., 2016) and humans (Adhikari et al., 2019) and human visual contrast discrimination (Zele et al., 2019b) potentially through retrograde feedback networks from melanopsin cells to outer retina (Sekaran et al., 2003; Zhang et al., 2008). The vision and pupil control pathways share retinal photoreceptors but are different in that ipRGCs entirely form the afferent pupil control pathway in mice (Güler et al., 2008) and non-human primates (Ostrin et al., 2018). Here we measure the cone-directed PLR during continuous light adaptation with high or low melanopic excitation to determine whether the melanopsin influence on cone signalling extends to the pupil control pathway.

2.   Materials and methods

2.1. *Participants and ethics statement*

Three male observers (age; O1, 30 yrs; O2, 37 yrs; and O3, 44 yrs) were recruited to participate in the study. Two observers (O1 and O2) were authors; O3 was an experienced psychophysical observer who was naïve to the purpose of the experiments. All protocols were carried out in accordance with the Queensland University of Technology Human Research Ethics Committee approval (no.: 1700000510) and followed the tenets of the Declaration of Helsinki. Informed written consent was obtained from all participants. A comprehensive ophthalmic examination was conducted on each observer, including the assessment of visual acuity (Bailey-Lovie Log MAR Chart), contrast sensitivity (Pelli-Robson Chart), colour vision (Ishihara pseudoisochromatic plates and L'anthony Desaturated D-15 Test), intraocular pressure (Icare® ic100, Icare Finland Oy, Vantaa, Finland) and fundus examination with fundus photography (Canon non-Mydriatic Retinal Camera, CR-DGi, Canon Inc.) and optical coherence tomography (RS-3000 OCT RetinaScan Advance, Nidek Co. Ltd., Tokyo, Japan). All participants had best corrected visual acuity better than 6/6, trichromatic colour vision, and no ocular and systemic disease.

2.2. *Apparatus, calibrations, and pupil recording*

In Experiment 1, photoreceptor bleaching was performed with a halogen lamp (17.7 x 12.5 cm; 131° x 115° visual angle at 4 cm) (Fig. 1) producing a broadband spectrum (CIE illuminant A, 1.3×10^{-5} Watts.cm^{-2}.s^{-1}, 39,400 cd.m^{-2}, 123,716 photopic Td with ~2 mm pupil diameter; correlated colour temperature = 2,788 K). To measure the post-bleach recovery of photoreceptor-directed pupil light responses (PLR), a separate 5-primary photostimulator having a 12-bit resolution and a 488 Hz high frequency limit was used to independently control the excitation of L-, M-, and S-cone opsins, rhodopsin and melanopsin (Cao et al., 2015). The photostimulator consists of five primary lights formed by combining light emitting diodes (LEDs) and narrow-band interference filters with peak wavelengths (full widths at half maximum) at 456 nm (10 nm), 488 nm (11 nm), 540 nm (10 nm), 594 nm (14 nm) and 633 nm (15 nm) (Cao et al., 2015). The primary lights' outputs are combined using fibre optic cables and a spatial homogeniser and focused by a field lens at the plane of a 2 mm artificial pupil in Maxwellian view creating a 30° circular field (Fig. 1). A central 10.5° macula blocker is used to avoid photo-absorption by the macular pigment. A small hole (<1 min of arc) in the centre of this macular blocker provides a fixation point. The light outputs are controlled by an LED driver (TLC5940) and an Arduino microcontroller (Arduino Uno SMD R3, Model A000073) by using a customised software (Xcode, Version 3.2.3, 64-bit, Apple, Inc., Cupertino, CA, USA) on Apple MacPro Quadcore Intel computer (Mac OS X, Version 10.6.8) (Adhikari et al., 2019; Zele et al., 2019a; Zele et al., 2018).

The spectral outputs and CIE 1964 10° chromaticity coordinates of the five primary lights were measured with a SpectraScan® Spectroradiometer PR-655 (Jadak – A Novanta Co., North Syracuse, NY, USA). The luminance outputs were measured with a calibrated radiometer (ILT1700 Research Radiometer; International Light Technologies, Inc., Peabody, MA, USA). The excitations of LMS cones, rods and melanopsin cells were calculated based on CIE 1964 10° standard observer cone fundamentals (Smith & Pokorny, 1975), CIE 1951 scotopic luminosity function, and melanopsin spectral sensitivity function (Adhikari et al., 2015; al Enezi et al., 2011), respectively. For an equal energy spectrum light at 1 photopic Td,

134 the photoreceptor excitation relative to photopic luminance with a 2:1 L:M cone ratio is L-cone
135 (l) = 0.6667, M-cone (m) = 0.3333, S-cone (s) = 1, rhodopsin (r) = 1 and melanopsin (i) = 1.
136 To obtain the maximum instrument gamut, we used an orange appearing adapting background
137 with the following relative photoreceptor excitations: l = 0.752, m = 0.248, s = 0.105, r = 0.319,
138 and i = 0.235 for Experiment 1 (Zele et al., 2018). In Experiment 2, we examined the effect of
139 melanopsin adaptation on cone-driven pupil responses by implementing an adapting
140 background with low (0.195) or high (0.245) melanopsin excitation (i) while retaining the same
141 *smlr* photoreceptor excitations as in Experiment 1.

142 To correct for the effect of individual differences in photoreceptor spectral
143 sensitivities and pre-receptoral filtering on silent-substitution paradigms (Pokorny et al., 2004;
144 Sun et al., 2001), the differences were estimated using Heterochromatic Flicker Photometry
145 (HFP). The sensitivity difference between an individual observer and the CIE 1964 10°
146 standard observer was then used to adjust the output of each primary light (for details, see
147 Adhikari et al., (2019)).

148 The PLR was recorded with an infrared (IR) video camera (640 × 480 pixels; 60
149 Hz; Point Grey FMVU-03MTM-CS; Richmond, BC, Canada) through a telecentric lens
150 (Computar TEC55, 55 mm telecentric lens; Computar, Cary, NC, USA) under IR illumination
151 (λ_{max} = 851 nm) (Feigl et al., 2011; Zele et al., 2019a; Zele et al., 2011). Chin rest, head restraint,
152 and temple bar stabilised the observer's head during pupil recording. The pupil videos were
153 processed offline to extract pupil diameter as a function of time using custom designed
154 MATLAB software (R2017b; Mathworks, Natick, MA) with artefacts due to eye blinks
155 removed and linear interpolated. The PLR amplitude was quantified with reference to baseline
156 pupil diameter defined as the average of the 100 ms pre-stimulus data immediately before
157 stimulus pulse onset (Fig. A.2 and A.4). The peak pupil constriction amplitude (% baseline
158 diameter) was defined as the smallest pupil diameter during the pulse stimulation, which we
159 call the 'PLR amplitude' hereafter. Measurements and analyses followed the Standards in
160 Pupillography (Kelbsch et al., 2019).

161

162 *2.3. Experiment 1: Bleaching adaptation of melanopsin photoreception*

163 To determine melanopsin regeneration kinetics, the right eye of the observer was
164 pre-exposed for 70 s to the halogen lamp. Immediately after offset of this bleaching light, the
165 test stimuli were presented to the right eye and the consensual PLR (mm diameter of the left
166 eye) was recorded during a 15 min recovery period (Fig. 1A). Bleaching adaptation is
167 conventionally quantified in the dark by varying stimulus intensity to obtain a criterion
168 response (Alpern & Campbell, 1963; Alpern et al., 1959; Alpern & Ohba, 1972; Hollins &
169 Alpern, 1973; Lamb & Pugh, 2004; Pianta & Kalloniatis, 2000; Thomas & Lamb, 1999; Wald
170 et al., 1950); however, the generation of photoreceptor-directed lights using the silent-
171 substitution technique requires a non-zero illumination level. Both Paupoo et al., (2000) and
172 Mahroo and Lamb (2004) have measured the bleaching adaptation responses of cone ERG in
173 response to repetitive but fixed-intensity red flashes on a rod-saturating blue background (1700
174 scotopic Td). We therefore extended that approach to measure the PLR post-bleach recovery
175 using fixed-contrast melanopsin-directed pulses during steady photopic light exposure. Given
176 that melanopsin threshold response occurs at the mesopic to photopic transition in the visual
177 (Zele et al., 2019b; Zele et al., 2020b) and pupil pathways (Adhikari et al., 2015; Gamlin et al.,
178 2007), we applied a 2,000 photopic Td adaptation level. During post-bleach photopigment
179 regeneration, the effective stimulus contrast will increase gradually following offset of the

180 bleaching light thereby resulting in an increase in the PLR amplitude. The test stimuli were a
181 1 s rectangular pulse that alternated between a melanopsin-directed (23% Weber contrast,
182 rhodopsin, and LMS-cone silent) and an LMS-cone-directed increment (23% Weber contrast,
183 rhodopsin and melanopsin silent) generating 45 melanopsin and 45 LMS trials in one session
184 (Fig. 1A). The LMS-cone-directed stimulus had L-, M-, and S-cones modulated in phase to
185 produce a cone luminance signal and provided a control condition to directly compare our
186 outcomes with the published studies that evaluated dark adaptation of the photopic luminance
187 mechanism (Mahroo & Lamb, 2012; Pianta & Kalloniatis, 2000; Rushton & Henry, 1968).
188 Hereafter, we use the term 'cone-opsin' to indicate all three cone opsins and the cone-opsin
189 recovery kinetics derived from the LMS-cone-directed PLR (see Section 2.6) represent their
190 combined contributions to the luminance pathway. The 1 s stimulus pulse was preceded by a 2
191 s pre-pulse interval used to establish the baseline pupil diameter for each trial; this stimulus
192 was followed by a 7 s post-pulse interval to allow recovery to baseline pupil diameter before
193 starting the successive trial. The pre- and post-pulse intervals included photoreceptor-directed
194 temporal white noise (Hathibelagal et al., 2016) that randomly modulates the LMS-cone and
195 rhodopsin excitations (40% Michelson contrast) without changing melanopsin excitation (Zele
196 et al., 2018) in order to desensitise inadvertent rod and cone photoreceptor intrusions during
197 presentation of melanopsin-directed lights including from penumbral cones (Zele et al., 2019a;
198 Zele et al., 2019b; Zele et al., 2018). Note that this photoreceptor-directed noise does not
199 produce any measurable pupil constriction (Zele et al., 2019a).

200   The post-bleach PLR measurement was conducted over at least 10 repeated
201 sessions per observer, on different days at similar times to minimise the effect of circadian
202 variation on melanopsin contributions to the PLR (Zele et al., 2011). The pre-bleach light-
203 adapted PLR in response to the melanopsin- and LMS-cone-directed stimuli was estimated
204 during a 2 min exposure to the same stimulus sequence (Fig. 1); at least 10 repeated estimates
205 were performed for each observer. The data from the repeated sessions were averaged. To
206 eliminate the effect of inter-individual variability in the pre-bleached PLR amplitudes on the
207 post-bleach PLR amplitudes, the post-bleach data were normalised to the respective averaged
208 pre-bleach data.
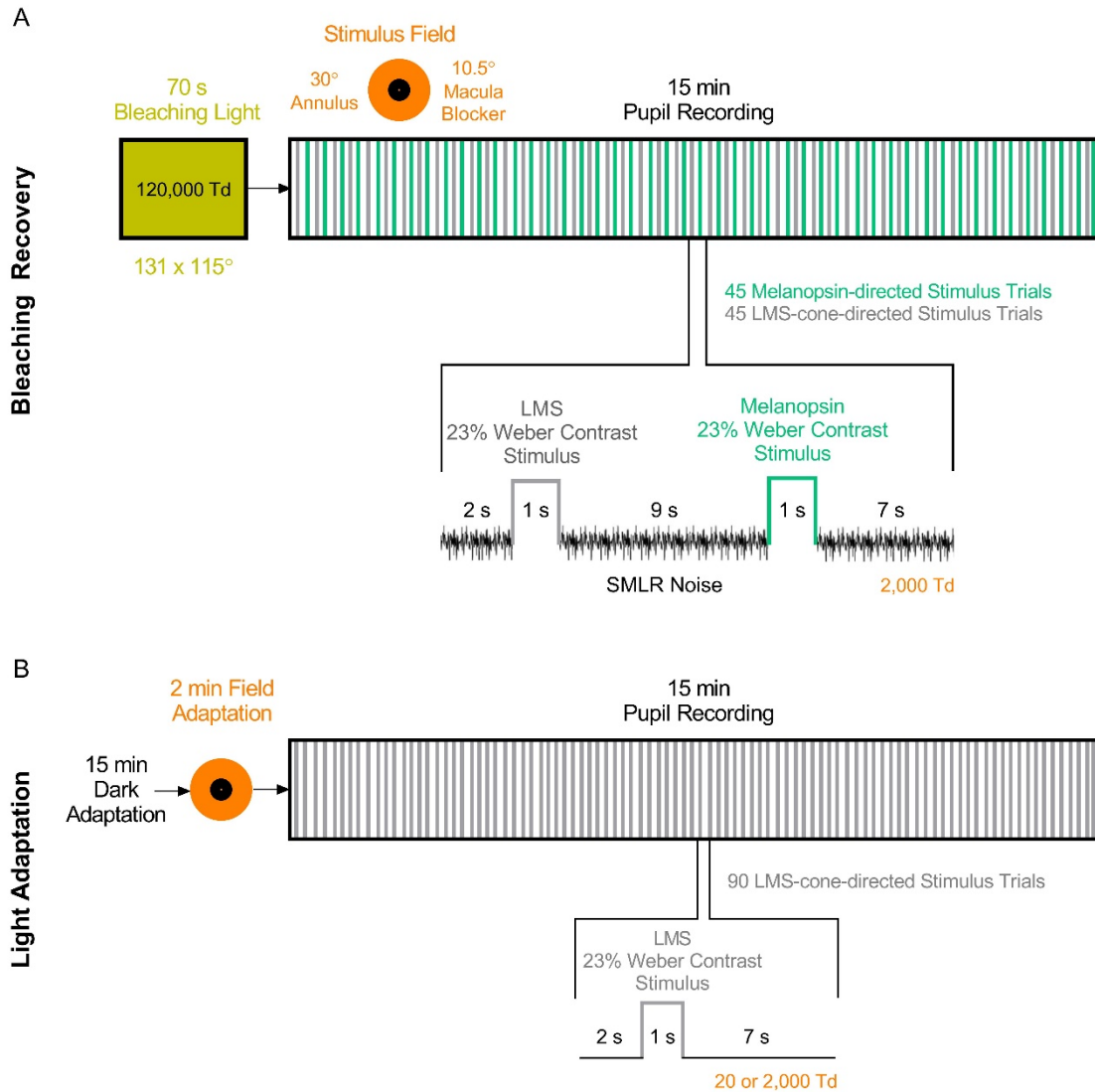
Fig. 1. (A) Bleaching adaptation pupillometry protocol (Experiment 1). Each pupillometry session included a 70 s exposure to a bleaching light and a 15 min continuous pupil recording. The PLR was recorded in response to a repetitive and interleaved stimulus window including a 1 s incremental pulse stimulus (melanopsin-directed or LMS-cone-opsin-directed) preceeded by a 2 s pre- and followed by a 7 s post-pulse interval with temporal white noise that modulated the LMS-cone and rhodopsin excitations (SMLR). Forty-five melanopsin-directed and 45 LMS-cone-directed stimulus pulses were presented during one 15 min session. (B) Light adaptation pupillometry protocol (Experiment 2). Each session included a 15 min dark adaptation, a 2 min adaptation to the background light, and a 15 min continuous pupil recording. The stimulus sequence was the same as in (A) except that the 1 s incremental pulse was always LMS-cone-directed and noise was not applied.

223   *2.4. Experiment 2: Effect of melanopsin adaptation on cone function*

224   To determine the influence of melanopsin adaptation on cone inputs to the pupil
225   control pathway, the PLR to LMS-cone directed incremental pulses (23% Weber contrast) was
226   measured during 15 min of continuous light adaptation to an adapting background (Fig. 1B)
227   with either high ($i = 0.245$) or low ($i = 0.195$) melanopsin excitation, but with the same cone
228   and rhodopsin excitations (and photopic luminance). There was a 25% difference in
229   melanopsin excitation between the two conditions. The adaptation level was either photopic
230   (2,000 Td) or mesopic (20 Td), with the latter forming the control condition because it is below
231   the melanopsin threshold level (Zele et al., 2019b). The stimulus sequence was the same as in
232   Experiment 1 except that temporal white noise was not required because the test pulses were
233   always LMS-cone directed (Fig. 1B). To eliminate any effect of pre-exposure to light, the
234   observers dark adapted for 15 min before Experiment 2. The test sequence started following a
235   2 min adaptation period to the background light. At least 5 repeated estimates were conducted
236   for each observer; the data from the repeated sessions were averaged.

237

238   *2.5. Photopigment bleach estimation*

239   The photopigment bleach was estimated following the framework provided by
240   Hollins and Alpern (1973) and Thomas and Lamb (1999) where the fraction of photopigment
241   bleached '*B*' is estimated as,

242    $$B = \frac{I}{I+I_p}\left(1 - exp\left(-\left(1+\frac{I}{I_p}\right)\frac{t_o}{\tau}\right)\right)$$ (1)

243   and t_o is the light exposure duration (70 s), I is the retinal illumination of the
244   bleaching light with a 2 mm pupil (123,716 photopic Td for cones and 307,929 scotopic Td for
245   rods, where scotopic Td = 2.489 * photopic Td (Wyszecki & Stiles, 1982)). Parameter I_p is the
246   steady-state equilibrium retinal illumination (when the rate of bleaching is equal to the rate of
247   regeneration) that bleaches half the pigment (4.3 log photopic Td for cones and 4.3 log scotopic
248   Td for rods) (Alpern, 1971; Rushton & Henry, 1968; Thomas & Lamb, 1999), and τ is the time-
249   constant of pigment regeneration (1.5 min for the cone-opsins and 7 min for rhodopsin)
250   (Alpern, 1971; Coile & Baker, 1992). A 70 s exposure to the broadband halogen lamp produced
251   86% cone-opsin bleach and 88% rhodopsin bleach. Melanopsin bleach estimation is described
252   in Section 2.6.

253

254   *2.6. Model fit for the post-bleach pupil light response recovery*

255   Measured raw pupil light response (PLR) amplitudes were plotted as a function of
256   time to determine the post-bleach PLR recovery. It was assumed that the post-bleach PLR
257   recovery is determined by photopigment regeneration as previously reported (Alpern & Ohba,
258   1972). The PLR recovery data were described using a first order exponential function that was
259   fitted using a least-squares fitting algorithm where the regeneration of the photopigment *P(t)*
260   at time *t* is defined by Eq. (2), where

261    $$P(t) = 1 - Bexp(-t/\tau)$$ (2)

262 and B is the initial bleaching level (see Section 2.3.1). Parameter $P(t)$ was replaced
263 with the normalised PLR amplitude data in the fitting. For the LMS-cone data, B was calculated
264 as described above (Eq. (1)) and τ was varied to optimise the best model fit. Given there is no
265 available estimate of melanopsin bleaching, both B and τ were varied for the model fit to
266 estimate the melanopsin bleach level. The B and τ values so derived were used in Eq. (1) to
267 calculate the steady-state retinal illumination I_p required to bleach half of the melanopsin
268 photopigment.

269 Conventionally, it is assumed that cone-opsin and rhodopsin regeneration follows
270 a first-order exponential defined by τ (Hollins & Alpern, 1973; Rushton & Henry, 1968) which
271 is dependent on the photopigment bleach level (Burns & Elsner, 1985; Paupoo et al., 2000;
272 Smith et al., 1983). Given that an alternate "rate-limited" model of photopigment regeneration
273 has been proposed based on the recovery of the photopic ERG a-wave amplitudes (Lamb, 1981)
274 where the initial rate of regeneration during ~6 min post-bleach is independent of bleach level
275 (Mahroo & Lamb, 2012) and steeper than in the exponential model, a rate-limited model was
276 also used to describe the data. The model was defined by Eq. (3), where

277
$$\mathrm{P}P(t) = 1 - K_m W\left(\tfrac{B}{K_m} exp\left(\tfrac{B}{K_m}\right) exp\left(-\tfrac{1+K_m}{K_m} vt\right)\right) \tag{3}$$

278 and $P(t)$ is the fraction of photopigment regeneration at time t (min), v is the initial
279 rate of response recovery (min^{-1}), and K_m is a semi-saturation constant at which recovery
280 reaches its maximum rate (Lamb, 1981). For melanopsin, parameter B was derived from the
281 exponential model fit.

282

283 *2.7. Precision of the photoreceptor isolation*

284 Photoreceptor isolation was confirmed through four control experiments conducted
285 in accordance with previous methods: (1) Rhodopsin-directed incremental pulses (18% Weber
286 contrast, 500 ms, 5 Td adaptation level) were visible only after ~4 min of dark adaptation post-
287 bleach. (2) Temporal colour matching of a cone-directed pulse (test; 18% Weber contrast) with
288 a rhodopsin-directed pulse (reference; 18% Weber contrast) required an increase in S/(L+M)
289 and (L+M) but a decrease in L/(L+M) in agreement with previous studies (Cao et al., 2005;
290 Cao et al., 2008a; Cao et al., 2008b). (3) At 0.2 Td, the rod critical flicker frequency was 15.8
291 Hz, consistent with the literature (Cao & Lu, 2012; Conner, 1982; Conner & MacLeod, 1977;
292 Teikari et al., 2012; Zele & Cao, 2015) whereas cone-directed flicker was invisible; (4) At 0.2
293 Td, rhodopsin-directed pulses produced a clear transient PLR at the pulse onset whereas cone-
294 directed pulses elicited no PLR.

295 The narrowing of the photoreceptor spectral nomograms with photopigment
296 bleaching (Dartnall, 1962) may introduce inaccuracies in estimated photoreceptor excitations
297 calculated using spectral nomograms determined in the absence of photopigment bleaching.
298 We therefore estimated the inadvertent luminance (LMS-cone) and chromatic (L-M) intrusions
299 in the melanopsin-directed incremental pulse that could arise from the narrowing of the spectral
300 sensitivities due to the bleaching. It was assumed that the broadband halogen spectrum would
301 cause a similar narrowing in all opsin nomograms as calculated using the estimates provided
302 by Dartnall (1962). The photopigment bleach levels during the 15 min post-bleach recording
303 period was estimated using Eq. (2) for the cone-opsins, rhodopsin and melanopsin. These
304 estimated photopigment spectra were used to calculate new theoretical *smlri* photoreceptor

305   excitations for generating a melanopsin pulse at each post-bleach time to compare with the
306   *smlri* excitations used in the main experiment. For this study, potential intrusions from cone
307   pathways are important. Cone-inputs to the inferred magnocellular and parvocellular pathways
308   are up to 10X more sensitive than melanopsin photoreception (Zele et al., 2018) and so small
309   cone intrusions can contaminate melanopsin-directed PLRs (Zele et al., 2019a). The difference
310   in the *smlri* excitations between the unbleached and bleached states were therefore calculated
311   to estimate the level of intrusion of potential achromatic (i.e., +L+M+S) or chromatic signals
312   (i.e., +L-M) in the putative melanopsin-directed pulse during photopigment bleach recovery.

313   This analysis shows that the theoretical melanopsin-directed pulse used in the main
314   experiment will introduce an estimated maximum -8.5% Weber contrast LMS-cone intrusion
315   and a +4.3% L-M-cone intrusion immediately post-bleach (time 0 min) (Fig. 2). These
316   intrusions are suprathreshold for the cone pathways (Zele et al., 2019b; Zele et al., 2018). With
317   increasing post-bleach recovery time, the level of cone intrusion decreases and is below the
318   respective cone pathway detection threshold at ~1 min for LMS and ~4 min for L-M; that the
319   stimulus is not isoluminant with the background means the predominant cone-intrusions are
320   achromatic signals during the initial ~1 min of the bleach recovery. Our application of the cone-
321   and rhodopsin-directed temporal white noise during the pre- and post-pulse periods (Fig. 1)
322   further limits the effect of non-melanopsin photoreceptor intrusions, including those from
323   penumbral cones (Horiguchi et al., 2013; Spitschan et al., 2015; Zele et al., 2018). Control
324   experiments in one observer (O1) demonstrated that in the absence of the noise, the
325   melanopsin-directed PLRs showed a cone-like post-bleach recovery of the PLR (see Results)
326   corroborating our published findings that noise desensitises cone intrusions in melanopsin-
327   directed pupil light responses (Zele et al., 2019a). Moreover, the pupil constriction threshold is
328   0.14 to 0.9 log units higher than for vision (Burke & Ogle, 1964) and therefore the estimated
329   cone intrusions due to photopigment bleaching would have lower interference in the
330   melanopsin-directed PLR. That any cone photoreceptor intrusion has a minor effect on the
331   outcomes is evident in the post-bleach melanopsin-directed PLR which shows the characteristic
332   slow and sustained pupil constrictions (see Results), consistent with previous reports (Zele et
333   al., 2019a).
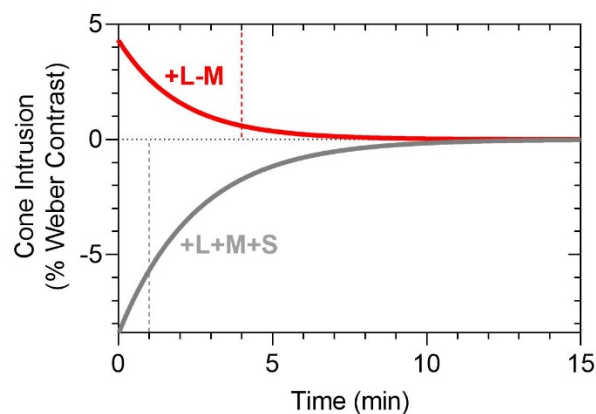
334

335   **Fig. 2.** Predicted time-course of cone intrusions in post-bleach melanopsin-directed pulse.
336   Achromatic (+L+M+S; grey line) and chromatic (+L-M; red line) cone intrusions (% Weber
337   contrast) in the melanopsin-directed incremental pulse (23% Weber contrast at 2,000 Td)
338   brought about by changes in the photoreceptor spectral nomograms due to photopigment
339   bleaching. The horizontal dotted line indicates no cone intrusion. Negative values indicate
340   decremental Weber contrasts from the adaptation level and the positive values indicate

341   incremental contrasts. The vertical dashed lines indicate the post-bleach times when the cone
342   intrusions are below the respective chromatic and achromatic visual detection thresholds.

343

344   *2.8. Statistical Analysis*

345   Statistical analyses were conducted using GraphPad Prism (GraphPad Software,
346   Inc., CA, USA). The data frequency distributions were estimated using the D'Agostino and
347   Pearson omnibus normality test. In Experiment 1, the best-fitting non-linear exponential and
348   rate-limited models were used to describe the post-bleach recovery of the PLR. Goodness of
349   fit was evaluated using a Chi-square test ($P > 0.05$). In Experiment 2, the PLR amplitudes over
350   time were compared between the low and high melanopsin excitation conditions by comparing
351   the slopes and intercepts of the best-fitting linear regressions (F-test, confidence interval =
352   95%, $p < 0.05$). Frequency distributions of the PLR amplitudes were plotted using a Gaussian
353   function defined by Eq. (4) where

354
$$YY = A * exp\left(-0.5 * \left(\frac{X-Mean}{SD}\right)^2\right) \tag{4}$$

355   and amplitude *A* is the height of the centre of the distribution in *Y* units, *X* is the
356   PLR amplitude (%), *Mean* is the average of the PLR amplitudes (%), and *SD* is the standard
357   deviation (%).

358

359 **3.   Results**

360   *3.1. Experiment 1: Bleaching adaptation of melanopsin inputs to pupil light response*

361   Melanopsin photopigment bleaching and regeneration kinetics were determined
362   post-exposure to a 123,716 photopic Td light by tracking the time-course of recovery of the
363   PLR amplitude in response to a melanopsin photoreceptor-directed pulse and compared to
364   contrast-matched LMS-cone-opsin-directed PLRs. The pre-bleach melanopsin-directed PLR
365   showed a slow constriction at pulse onset (latency to constriction = ~567 ms for the melanopsin
366   PLR and ~383 ms for the cone PLR) and a sustained constriction after pulse offset whereas the
367   LMS-cone-directed PLR showed a transient constriction at pulse onset with a rapid redilation
368   to the baseline after pulse offset (Fig. 3), consistent with previous reports (Zele et al., 2019a).
369   The melanopsin-directed PLR amplitude during pulse stimulation was 2.04 ± 0.23% (mean ±
370   standard error of the mean, SEM) compared to 6.57 ± 0.34% cone-directed PLR (Fig. 3). At 1
371   min post-bleach, the LMS-cone PLR amplitude was 67% lower (2.14 ± 0.21%) than the pre-
372   bleach baseline then progressively increased over time and recovered to the pre-bleach
373   amplitude (~6.6%) after ~9 min (Fig. 3). In contrast, at 1 min post-bleach the melanopsin PLR
374   amplitude was 32% lower (1.39 ± 0.19%) than the pre-bleached baseline then progressively
375   recovered to the pre-bleach amplitude (~2%) after ~11 min (Fig. 3). Figure 3 shows the pupil
376   traces at pre-bleach and those at 1, 2, 3, 4, 5, and 15 min post-bleach. Figure 4 shows all PLR
377   amplitudes extracted from the traces every 20 s both at pre-bleach and post-bleach.
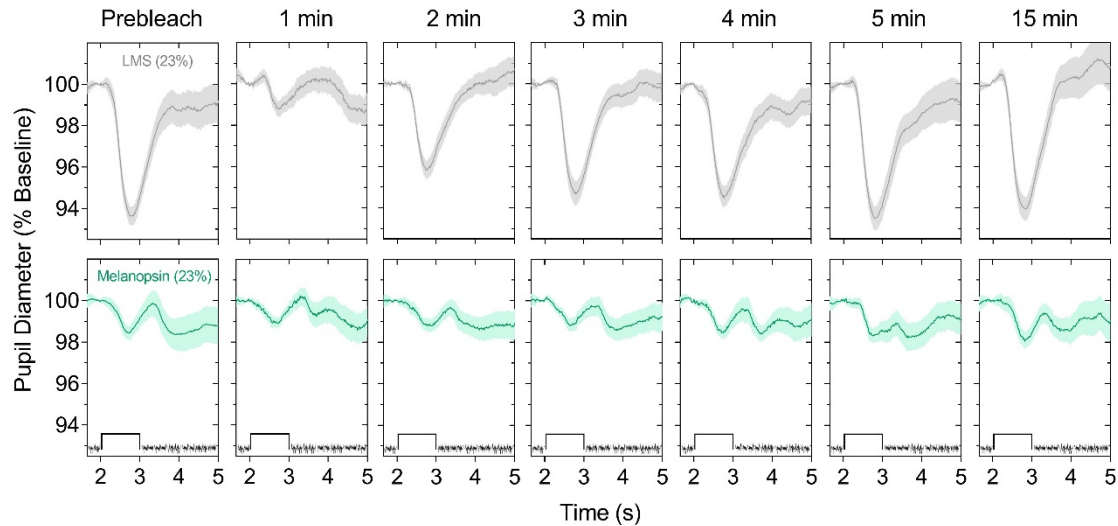
Fig. 3. Post-bleach recovery of melanopsin-directed PLR (green lines) and cone-directed PLR (grey lines). Light-adapted (2,000 Td) PLRs at pre-bleach (baseline) and selected post-bleach times show that the relative reduction in melanopsin-directed PLR following offset of a 123,716 photopic Td bleaching light is less than in cone-directed PLR amplitudes. Data show the average responses (± 95% confidence limits; shaded regions) from 3 observers. The 1 s stimulus pulse and temporal white noise are shown on the abscissa in the bottom row.

The post-bleach regeneration kinetics of melanopsin and cone-opsin were derived from the post-bleach PLR amplitudes normalised to the average pre-bleach amplitude (Fig. 4). Both the best-fitting exponential function (Eq. (2)) and rate-limited model (Eq. (3)) provided satisfactory goodness of fits to the time-course of regeneration (Cone-opsin; exponential: χ^2_{44} = 0.14 to 0.64 in 3 observers, sum of squared errors (SSE) = 0.118 to 0.570, p = 1; rate-limited: χ^2_{44} = 0.14 to 0.56, SSE = 0.096 to 0.525, p = 1; melanopsin; exponential: χ^2_{44} = 0.172 to 0.805, SSE = 0.168 to 0.785, p = 1; rate-limited: χ^2_{44} = 0.173 to 0.803, SSE = 0.166 to 0.757, p = 1). Therefore, only the exponential models are shown in Fig. 4 (lines). The three observers had similar post-bleach recoveries and therefore we computed the average time-course (fourth row, Fig. 4).

There are two phases during the initial post-bleach regeneration of cone-opsins with different τ values (Pianta & Kalloniatis, 2000); that our pupil data were collected with a low temporal resolution (10 s) in order to characterise the entire PLR recovery to baseline, only a single recovery phase was observed. For the melanopsin PLR, the average τ was 2.48 ± 0.01 min and the time to complete recovery (*T*) to the pre-bleach amplitude was 11.22 ± 0.11 min, 1.5X and 1.2X slower than for the cone PLR, respectively (τ = 1.68 ± 0.05 min; *T* = 9.11 ± 0.77 min) (Table 1). For the melanopsin post-illumination pupil response (PIPR) quantified at 1.8 s after pulse offset (Zele et al., 2019a), the post-bleach recovery was nearly identical to that for the melanopsin PLR, with τ = 2.48 min and *T* = 11.04 min on average (Fig. A.1). The estimated melanopsin bleach was ~43%, half of the cone-opsin bleach (86%). For direct comparison, we therefore re-measured the cone PLR recovery following 43% cone bleach (70 s exposure to a 22,600 photopic Td illumination using the same bleaching light) (Fig. 4, black circles and lines). With the percentage bleach matched, the cone PLR had ~3.4X faster τ (0.74 ± 0.01 min) and *T* (3.33 ± 0.00 min) than for the melanopsin PLR. The steady-state pupil size measured during the pre-pulse period (Fig. A.2) also recovered exponentially with a τ of ~4 min, 1.5X faster than reported for pupil recovery in the dark (Alpern & Campbell, 1963; Alpern & Ohba,

411   1972). This indicates that the post-bleach pupil size recovery under light adaptation is mediated
412   by all photoreceptor classes compared to the rod-mediated recovery measured in the dark.

413
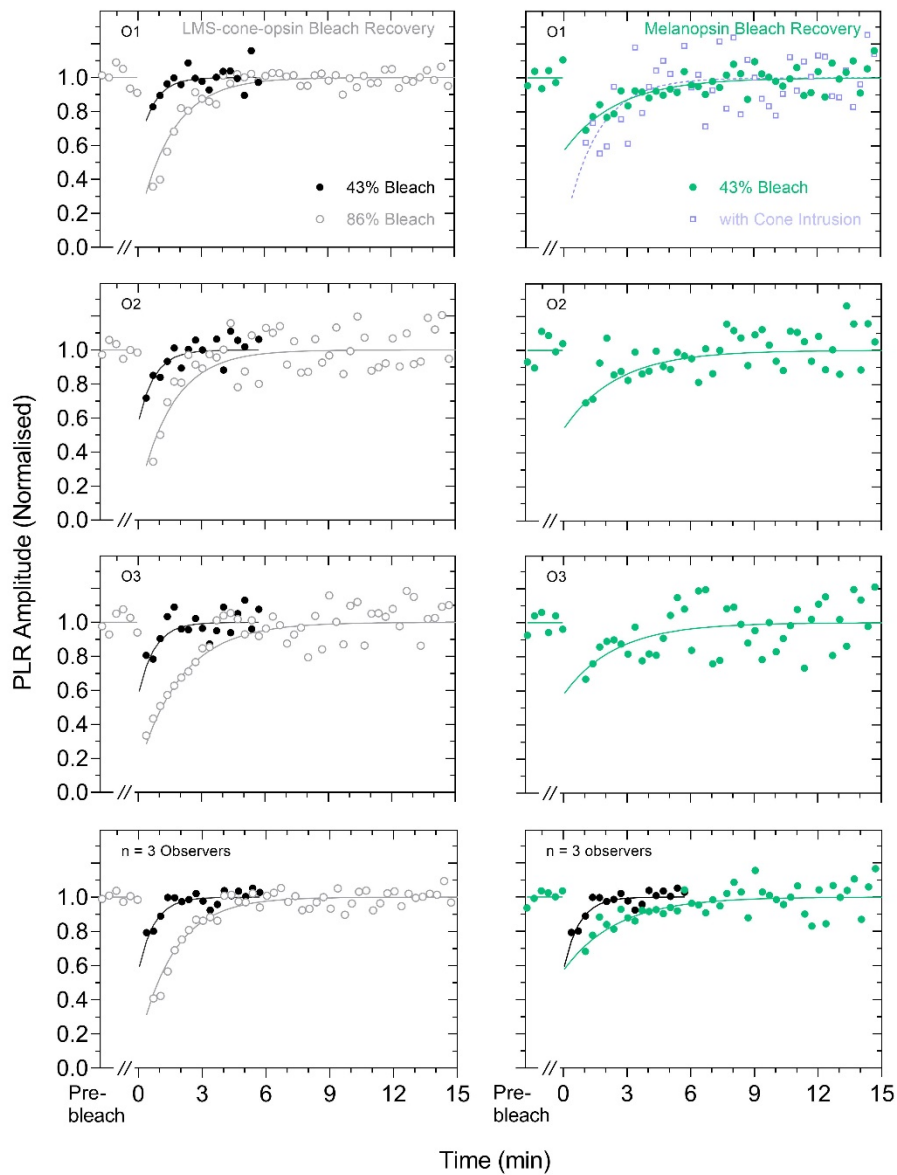
Fig. 4. Post-bleach PLR recovery of the melanopsin and cone pathways. The 123,716 photopic
Td broadband light (offset at time 0 min) bleaches 86% of the LMS-cone-opsin (left panels)
and 43% of the melanopsin (right panels). The light-adapted (2,000 Td) PLR amplitudes
sampled every 20 s during the 15 min post-bleach recovery are shown for three observers (O1,
O2, O3) for the LMS-cone-opsin (grey filled circles) and melanopsin-directed conditions
(green filled circles, with noise; unfilled blue squares (for O1), without noise). The black
unfilled circles represent the LMS-cone-opsin recovery following the melanopsin and cone-
opsin equated bleach (43%, see text for details). Bottom panels show the data averaged across
the three observers; the 43% cone bleach data (black unfilled circles) are also plotted in the
right panel for comparison with melanopsin (green filled circles). The post-bleach PLR
amplitudes are normalised to the pre-bleach amplitude (before time 0 min). The solid lines
indicate the best-fitting linear regressions (pre-bleach data) and first-order exponential models
(post-bleach data).

427

Table 1

Post-bleach regeneration time-constant (τ, min) and time to complete recovery (T, min) of melanopsin- and LMS-cone-opsin-directed PLRs.

431

Observer	Cone-opsin 86% Bleach		Cone-opsin 43% Bleach		Melanopsin 43% Bleach	
	τ	T	τ	T	τ	T
O1	1.63	8.33	0.72	3.33	2.50	11.33
O2	1.63	8.33	0.75	3.33	2.50	11.33
O3	1.78	10.67	0.75	3.33	2.45	11.00
Mean	1.68	9.11	0.74	3.33	2.48	11.22
± SEM	± 0.05	± 0.77	± 0.01	± 0.00	± 0.01	± 0.11

432

In order to provide a framework to calculate the melanopsin bleach level with lights of any irradiance and duration, we next estimated parameter I_p to apply in Eq. (1). Given that the photometrically measured luminance of a light does not represent the melanopsin spectral response, we derived melanopsin I_p for three different measurement units to define opsin specific excitations: 1) Photoreceptor effective Td (Rebec & Gunde, 2014), 2) photoreceptor effective photons.cm^{-2}.s^{-1} (Revell & Skene, 2007), and 3) photoisomerisations.photoreceptor^{-1}.s^{-1} (Lyubarsky et al., 2004). Parameter I_p for the cone-opsin and rhodopsin in Td was defined in Section 2.5; here we estimated it for the latter two units. Parameter I was calculated for the different light units as described in the following (Table 2).

To calculate melanopic effective Td, photopic Td was multiplied by a melanopic action factor (A_{cv}) (Rebec & Gunde, 2014), defined as

$$A_{cv} = \frac{\int_{400}^{700} C(\lambda)S(\lambda)d(\lambda)}{\int_{400}^{700} V(\lambda)S(\lambda)d(\lambda)} \tag{5}$$

where $C(\lambda)$ is melanopic spectral sensitivity, $V(\lambda)$ is photopic 10° luminosity function, and $S(\lambda)$ is spectral output of the light source.

To express a light in terms of photon absorptions for a specific opsin, photoreceptor specific effective photon flux (φ) (Revell & Skene, 2007) was calculated by cross-correlating the spectral output of the light source $S(\lambda)$ with the photoreceptor spectral sensitivity $P(\lambda)$ corrected for pre-receptoral filtering (Jacobs & Williams, 2007; Revell & Skene, 2007) using Eq. (6), where

$$\varphi = \int P(\lambda)S(\lambda) \tag{6}$$

In this analysis, the photoreceptor spectral sensitivities were specified based on the CIE 1964 10° standard observer cone fundamentals (Smith & Pokorny, 1975), the CIE 1951 scotopic luminosity function, and melanopsin spectral sensitivity function (Adhikari et al., 2015; al Enezi et al., 2011). The cone-opsin effective photon flux for the L-, M-, and S-cones were combined using the relative weighting factors based on the ratio of L-cone, M-cone, and S-cone availability (L:M:S = 0.53:0.38:0.09) in the human retina (Dartnall et al., 1983).

459   To express a light in terms of the resultant rate of photoisomerisations in a
460 photoreceptor (Lyubarsky et al., 2004), photoisomerisations.photoreceptor^{-1}.s^{-1} (φ_p) was
461 calculated as,

462
$$\varphi_p = \varphi\left(\frac{A_p}{A_r}\right)a_c(\lambda) \tag{7}$$

463   where φ is effective photon flux (Eq. (6)), A_p/A_r is the ratio of pupil area (3.14
464 mm^2) to retinal area (1,094 mm^2) (Kolb et al., 1995), and $a_c(\lambda)$ is the collecting area of a single
465 photoreceptor. In this analysis, we adopt a 0.5 μm^2 area for rods (Nikonov et al., 2005; Nikonov
466 et al., 2006) and 1 μm^2 for cones (Naarendorp et al., 2010) averaged across the retina, and 5
467 μm^2 for melanopsin cells, with the assumption that melanopsin phototransduction occurs
468 uniformly over the entire cell surface (Do et al., 2009). Note that these photoreceptor areas are
469 obtained from mouse models and the calculations can be updated with human and non-human
470 primate data when available.

471

472 **Table 2**

473 Photopigment specific excitations (I) produced by the bleaching light and half-bleaching
474 steady-state light levels (I_p) for all opsin types in three different light units.

475

Opsin	Log effective Td		Log effective photons.cm^{-2}.s^{-1}		Log photoisomerisations. photoreceptor^{-1}.s^{-1}	
	I	I_p	I	I_p	I	I_p
Cone-opsin	5.09	4.30	16.69	15.89	8.14	7.35
Rhodopsin	5.49	4.30	16.42	15.89	7.58	7.35
Melanopsin	4.76	4.54	16.29	16.10	8.45	8.25

476

477   The half-bleaching steady-state level (I_p), where photopigment bleach and
478 regeneration are at an equilibrium, was estimated at 4.54 log effective Td (equivalent to 16.10
479 log effective photons.cm^{-2}.s^{-1} or 8.25 log photoisomerisations.photoreceptor^{-1}.s^{-1}) for
480 melanopsin, which was higher than for the cone-opsin or rhodopsin (Table 2). Since we did not
481 measure the rhodopsin-directed PLR and I_p for rhodopsin in scotopic Td is approximately the
482 same as for cone-opsin in photopic Td (Alpern, 1971; Ripps & Weale, 1969; Rushton, 1961;
483 Rushton & Henry, 1968; Thomas & Lamb, 1999) (see Section 2.5), we assumed that I_p for
484 rhodopsin and cone-opsin is equivalent in opsin effective photons or photoisomerisations as
485 well (Table 2). Having evaluated the regeneration time-constant (τ) and the equilibrium retinal
486 illumination (I_p) for all opsin types, we then calculated the photopigment bleach (B) value for
487 a larger range of light levels above and below I_p (Fig. 5). With increasing opsin excitation,
488 there is an inverse sigmoid relationship as a function of the percentage of unbleached opsin. In
489 general, the melanopsin bleach with a broadband halogen light is less than for the cone-opsin
490 and rhodopsin for an opsin specific excitation (vertical slices in Fig. 5). In accordance with our
491 assumption of equivalent I_p for rhodopsin and cone-opsin in opsin effective light units, the

492 rhodopsin and cone-opsin bleach levels overlap when plotted as a function of opsin effective
493 units (Fig. 5B, C, D) but differ when plotted as a function of photopic Td (Fig. 5A).

494
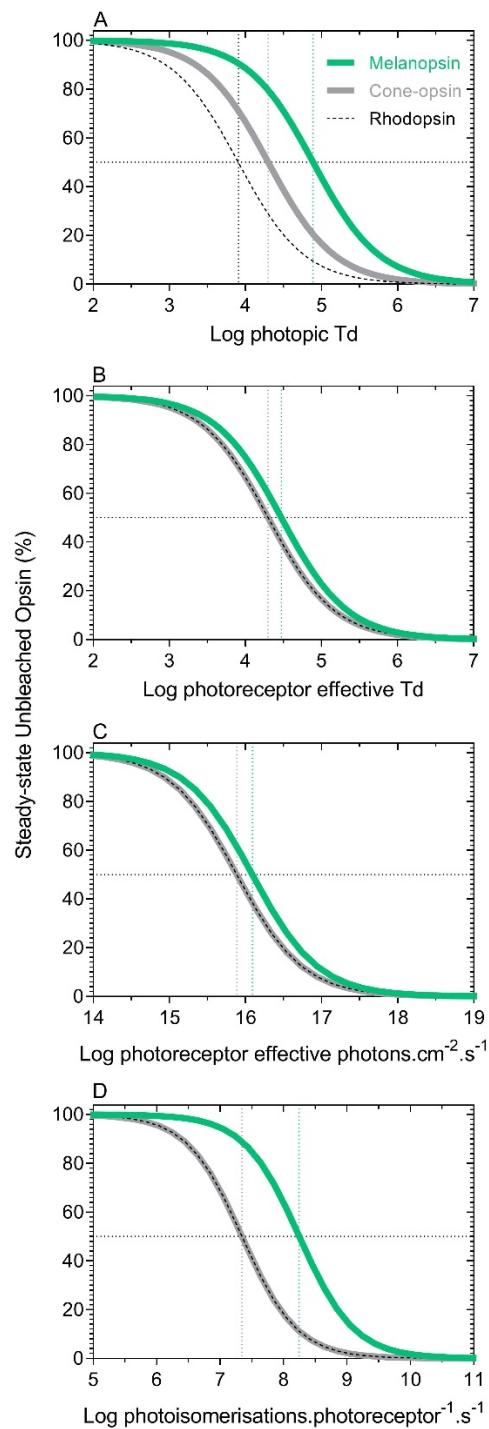
Fig. 5. Estimated photopigment bleach level as a function of opsin specific excitation in three different light units. Unbleached steady-state equilibrium photopigment percentage was calculated as a function of (A) photopic Td as well as opsin specific (B) effective Td, (C) photon flux, and (D) photoisomerisations for melanopsin (green line), cone-opsin (grey line), and rhodopsin (dashed black line - overlapping with cone-opsin). The horizontal dotted line indicates a 50% bleach and the vertical lines indicate the equilibrium retinal illumination (I_p).

501

3.2. Experiment 2: Effect of melanopsin adaptation on cone inputs to pupil light response

Having determined that melanopsin photopigment shows resistance to bleaching compared to cone-opsin and given the evidence that melanopsin excitation influences light-adapted cone functions in mouse models (Adhikari et al., 2019; Allen et al., 2014; Prigge et al., 2016; Zele et al., 2019b) as well as humans (Adhikari et al., 2019; Allen et al., 2014; Prigge et al., 2016; Zele et al., 2019b), we next evaluated whether melanopsin adaptation has any effect on cone contributions to PLR. Cone-directed PLR amplitudes were measured every 10 s during a 15 min adaptation period (90 pupil amplitude data points) to the continuously presented adapting field having either high ($i = 0.245$) or low ($i = 0.195$) melanopsin excitation (Fig. 6A, C). At a mesopic illumination (20 Td) below the melanopsin threshold (Zele et al., 2019b), cone PLR amplitudes did not differ between the high and low melanopsin excitation (Fig. 6A). On the other hand, at a photopic illumination (2,000 Td), cone PLR amplitudes increased by 10% with the high melanopsin excitation (Fig. 6C). Accordingly, the intercepts of the regression lines fitted to the PLR amplitudes over time were significantly different ($F_{1,177} = 54.75$, $p < 0.0001$) between the high and low melanopsin excitation conditions at 2,000 Td (Fig. 6C) but not at 20 Td ($F_{1,177} = 0.51$, $p = 0.48$) (Fig. 6A). The slopes of the regression lines were not significantly different from zero indicating that the LMS-cone-directed PLR was invariant during continuous light adaptation (Table 3). To determine whether the PLR amplitudes reported in Figure 6A and C are the direct consequence of the cone-directed stimulus pulse and not autonomic fluctuations in pupil size (Loewenfeld & Lowenstein, 1993; Zele & Gamlin, 2020), we analysed the pupil diameters at random times during the 2 s pre-stimulus epochs. The averaged baseline pupil diameters (mm) are shown in Fig. A.3. During the pre-stimulus epoch, there was a negligible difference in pupil diameter from the baseline (mean ± SEM, $0.01 \pm 0.01\%$) and independent of the adaptation level (Fig. A.3) indicating that the pupil constriction is a direct result of the LMS-cone-directed pulse stimulation.

527
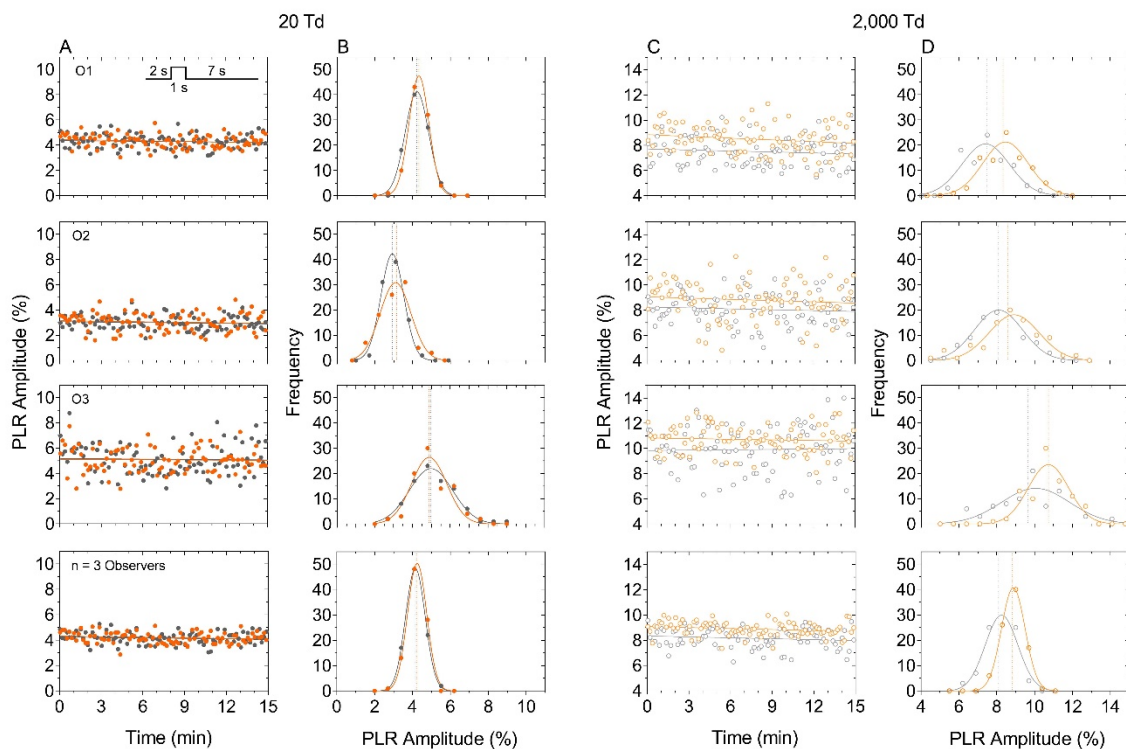
528 **Fig. 6.** Melanopsin light adaptation enhances the photopic but not mesopic cone-directed PLR.
529 (A) LMS-cone-directed PLR amplitudes measured during the 15 min light adaptation (20 Td)
530 under high-melanopsin excitation (orange filled circles) or low-melanopsin excitation (grey
531 filled circles). The stimulus window is schematically depicted in the top left panel. The solid
532 lines indicate the best-fitting linear regressions. (B) Frequency of occurrence of the PLR
533 amplitudes from Panel A sampled into 0.7% bins and fitted with Gaussian functions (solid
534 lines). The dotted vertical lines indicate the distribution means. (C) Cone PLR amplitudes
535 measured during the 15 min light adaptation (2,000 Td) under high-melanopsin excitation
536 (orange unfilled circles) or low-melanopsin excitation (grey unfilled circles). (D) Frequency of
537 occurrence of the PLR amplitudes from Panel C.

538 **Table 3**

539 Linear regression parameters for the cone-directed PLR amplitudes at 20 Td and 2,000 Td as
540 a function of adaptation time.

20 Td Mesopic Adaptation

Observers	High-melanopsin Excitation ($i = 0.245$)				Low-melanopsin Excitation ($i = 0.195$)			
	r^2	$F_{1,88}$	Slope	p	r^2	$F_{1,88}$	Slope	p
O1	0.02	1.86	-0.02	0.18	0.005	0.44	-0.01	0.51
O2	0.007	0.60	-0.01	0.44	0.009	0.78	-0.01	0.38
O3	0.001	0.06	-0.01	0.81	0.001	0.06	-0.01	0.81
Mean	0.01	0.84	-0.01	0.48	0.01	0.43	-0.01	0.57
± SEM	± 0.01	± 0.53	± 0.00	± 0.18	± 0.00	± 0.21	± 0.00	± 0.13

2,000 Td Photopic Adaptation

Observers	r^2	$F_{1,88}$	Slope	p	r^2	$F_{1,88}$	Slope	p
O1	0.03	2.96	0.03	0.09	0.01	0.93	0.03	0.34
O2	0.009	0.81	0.04	0.37	0.007	0.66	0.03	0.42
O3	0.005	0.44	0.03	0.51	0.001	0.06	0.04	0.81
Mean	0.01 ±	1.40	0.03	0.32	0.01	0.55	0.03	0.52
± SEM	0.01	± 0.79	± 0.00	± 0.12	± 0.00	± 0.26	± 0.00	± 0.15

541
542 To further characterise the enhancement of the cone-directed PLR with melanopsin
543 light adaptation, the frequency of occurrence of the PLR amplitudes was plotted as a function
544 of equal size bins (0.7%, chosen to enhance visualisation) (Fig. 6B, D) and modelled using
545 Gaussian functions (Table 4). The melanopsin enhancement of the cone-mediated PLR
546 amplitude under a photopic illumination (2,000 Td) was evidenced as a rightward shift of the
547 Gaussian frequency. Together, the regression analyses and frequency distributions indicated
548 that it is melanopsin adaptation that increases the cone-directed PLR in photopic illumination,
549 with no such effect in mesopic illumination below melanopsin threshold. Given the invariance
550 of cone-directed PLR during the 15 min light adaptation, the average responses were calculated
551 (Fig. 7).

552 **Table 4**

553 Gaussian distribution parameters of the frequency of occurrence of LMS-cone-directed PLR
554 amplitudes at 20 Td and 2,000 Td adaptation

20 Td Mesopic Adaptation

Observers	High-melanopsin Excitation ($i = 0.245$)				Low-melanopsin Excitation ($i = 0.195$)			
	Amplitude	Mean	SD	p	Amplitude	Mean	SD	p
O1	47.34	4.33	0.52	0.90	41.14	4.22	0.62	0.72
O2	30.80	3.09	0.82	0.06	42.13	2.92	0.61	0.31
O3	26.32	4.88	0.93	0.23	21.90	4.98	1.15	0.14
Mean	34.82	4.10	0.76	0.40	35.06	4.04	0.79	0.39
± SEM	± 6.39	± 0.53	± 0.12	± 0.26	± 6.58	± 0.60	± 0.18	± 0.17

2,000 Td Photopic Adaptation

Observers	Amplitude	Mean	SD	p	Amplitude	Mean	SD	p
O1	21.23	8.46	1.20	0.54	21.10	7.45	1.23	0.20
O2	18.08	8.91	1.33	0.24	19.96	8.09	1.28	0.64
O3	23.45	10.73	1.07	0.76	14.08	10.05	1.81	0.73
Mean	20.92	9.37	1.20	0.51	18.38	8.53	1.44	0.52
± SEM	± 1.56	± 0.69	± 0.08	± 0.15	± 2.18	± 0.78	± 0.19	± 0.16

555

556
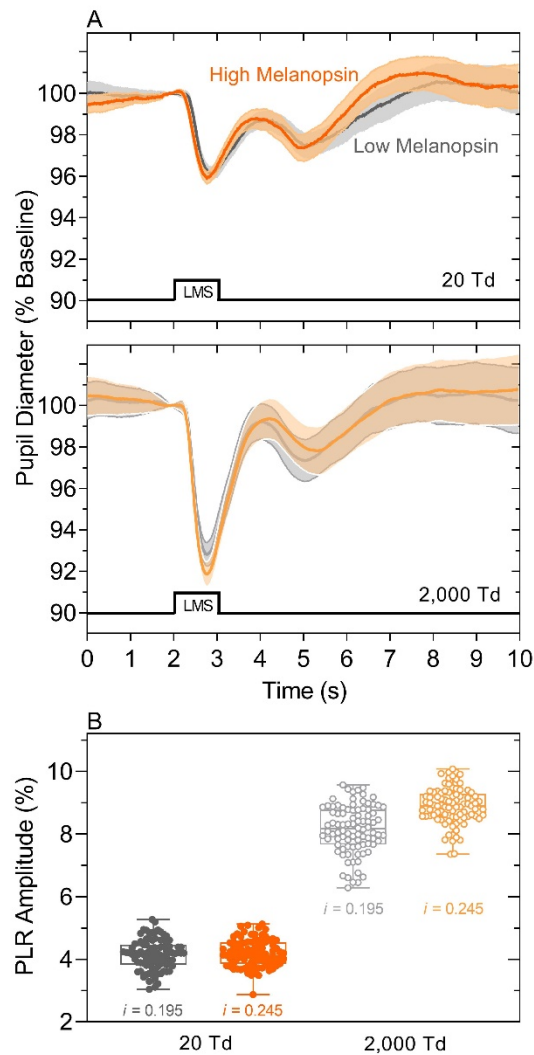
Fig. 7. Cone-directed pupil response amplitudes are enhanced under photopic melanopsin light
adaptation. (A) LMS-cone-directed pupil light responses (mean ± 95% confidence intervals)
under high melanopsin (orange lines) and low melanopsin excitation (grey lines) at mesopic
(20 Td, upper panels) and photopic adaptation levels (2,000 Td, lower panels). The stimulus
sequence is depicted along the abscissa (black lines). (B) The pupil light response (PLR)
amplitudes extracted from traces in (A) using the same colour coding (n = 3 observers).

563

4. Discussion

Exposure to an intense broadband light (70 s, ~120,000 Td) bleaches 43% (parameter
B, Eq (1) & (2)) of the available melanopsin photopigment compared to 86% of cone-opsin
and 88% of rhodopsin (Fig. 4). The post-bleach recovery of melanopsin as estimated from the
intrinsic pupil light response (PLR) followed an exponential regeneration time course with a
2.5 min time constant (τ) and complete recovery at 11.2 min (T) (Table 1). Compared to cone-
opsin, the melanopsin photopigment regeneration was ~3.4X slower under conditions having
equated pigment bleach levels; it would be ~1.2X faster than the reported rhodopsin
regeneration (Pugh, 1975). Using the classic bleach calculation equations with the B and τ (Eq.

573 (1)) (Hollins & Alpern, 1973; Mahroo & Lamb, 2004; Thomas & Lamb, 1999), the half-
574 bleaching light level (I_p) was estimated at 4.47 log melanopic Td (16.10 log melanopsin
575 effective photons.cm^{-2}.s^{-1}; 8.25 photoisomerisations.photoreceptor^{-1}.s^{-1}). With parameters τ and
576 I_p, the melanopsin bleach levels can be estimated for photometrically and radiometrically
577 quantified lights. It was then determined that continuous exposure (15 min) to photopic
578 adapting lights with a higher melanopsin adaptation can increase the cone-directed pupil
579 constriction amplitude by ~10% (Fig. 6, 7). Compared to cone-opsin and rhodopsin
580 regeneration, our findings suggest that melanopsin light adaptation might require alternate
581 avenues for the pigment regeneration and to minimise bleaching, including its strong
582 chromophore-opsin bond, photoconversion to a meta-state (Sexton et al., 2012), and bistability
583 (Mure et al., 2009) or tristability (Emanuel & Do, 2015). The melanopsin enhancement of cone
584 inputs to the PLR is in line with the reports of melanopsin-mediated enhancement of cone
585 inputs to vision (Zele et al., 2019b), together indicating that melanopsin activity can modulate
586 photopic cone signalling along both the visual and non-visual retina-brain axes.

587   For the halogen light used in this study, even though the effective photons for
588 melanopsin were 0.4 log units lower and the photoisomerisations were 0.3 log units higher than
589 for the cone-opsins (Table 2), the estimated melanopsin bleach was ~½ of the cone-opsin
590 bleach. On the other hand, even though the effective photons and photoisomerisations were
591 different between cone-opsins and rhodopsin, the cone-opsin and rhodopsin bleaches were
592 identical. The effective photons and photoisomerisations therefore do not explain the inter-
593 opsin bleach differences. The lower melanopsin bleach level could result due to a combination
594 of four of its unique properties. Firstly, the bond between the chromophore molecule and opsin
595 protein is stronger in melanopsin than in cone-opsins and rhodopsin (Sexton et al., 2012) and
596 so it may remain mostly intact during phototransduction, therefore minimising bleaching.
597 Secondly, melanopsin may possess a bistable (Mure et al., 2009) or tristable (Emanuel & Do,
598 2015) property wherein shorter wavelengths initiate phototransduction of 11-cis retinal to all-
599 trans retinal whereas longer wavelengths re-isomerise all-trans retinal to the active 11-cis
600 retinal (Mure et al., 2009). It may be that the shorter wavelengths in the broadband bleaching
601 light initiated melanopsin phototransduction with the longer wavelength spectral component
602 inducing re-isomerisation, thereby reducing or nullifying the resultant bleach effects at light
603 offset. The bleaching light had more long wavelength energy than short wavelength energy;
604 however, a light (e.g., daylight) with more short wavelength energy would produce more
605 melanopsin bleach than with the halogen light, due to higher photon capture probability and
606 lower long wavelength induced re-isomerisation. To test this proposal and quantify the relative
607 contributions of melanopsin bistability to limiting its bleach; our estimated τ and I_p parameters
608 will enable future studies to quantify melanopsin bleaching and regeneration for lights with
609 different spectral properties. Thirdly, melanopsin may convert to a meta-state after the first
610 level of phototransduction (Sexton et al., 2012), similar to the rhabdomeric photopigment
611 (Hillman et al., 1983), and so it can still capture photons. With these alternate avenues
612 potentially important for resisting photopigment bleaching, melanopsin regeneration may also
613 only partially rely on the RPE-based photocycle, as has been evidenced in mice (Zhao et al.,
614 2016). We observed that melanopsin regeneration had a longer time constant than the cone-
615 opsin (Table 1) indicative of a delayed replenishment of 11-cis retinal, possibly because
616 melanopsin expressing ipRGCs are further from the RPE than cone photoreceptors. Finally,
617 the ~10^{4}X lower melanopsin pigment density than the cone-opsin and rhodopsin (Do et al.,
618 2009) leads to a 10^{6}X lower photon capture probability and potentially a lesser photopigment
619 bleach for an equivalent opsin specific excitation level. The partial resistance of melanopsin to
620 photic bleaching observed in our study might facilitate its irradiance signalling during
621 prolonged light exposure (Wong, 2012). This unique photon counting characteristic is

622 necessary for circadian photoentrainment to encode irradiance changes during the 24 hour day-
623 night cycle without saturating (Berson et al., 2002) as well as to control the pupil size during
624 steady illumination (McDougal & Gamlin, 2010; Zele et al., 2019a) and input to the
625 photophobia pathway during daylight illumination (Zele et al., 2020a), and to optimise cone-
626 mediated vision to the environmental illumination (Zele et al., 2019b).

627 Melanopsin adaptation increased the cone PLR amplitudes by 10%, which is equivalent
628 to reducing the pupil threshold contrast by 10%. Transient changes in illumination are signalled
629 by extrinsic cone-inputs to the pupil control pathway to which melanopsin provides minimal
630 direct contributions (Gooley et al., 2012; McDougal & Gamlin, 2010; Zele et al., 2019a)
631 whereas melanopsin drives the steady-state pupil diameter during extended light adaptation
632 (McDougal & Gamlin, 2010; Zele et al., 2019a). The constrictions were larger with the same
633 contrast cone-directed pulse when melanopsin excitation was higher in the adapting light
634 indicating that melanopsin signalling enhances cone sensitivity to PLR to keep the pupil small
635 during transient increases in illumination possibly to minimise optical aberrations and increase
636 image contrast. The melanopsin-mediated enhancement was constant in magnitude during the
637 15 min light adaptation at 2,000 Td (Fig. 6), perhaps related to the constant and dominant
638 contributions of intrinsic melanopsin signalling to the PLR during prolonged illuminations
639 (McDougal & Gamlin, 2010; Zele et al., 2019a). Evidence suggests melanopsin activation also
640 enhances cone-directed contrast discrimination in the visual pathway in humans (Allen et al.,
641 2019; Zele et al., 2019b), and influences the cone ERG in mice (Allen et al., 2014; Prigge et
642 al., 2016) and humans (Adhikari et al., 2019) and RGC activity in mice (Schmidt et al., 2014).
643 The retina is common in all of these pathways; the source of the melanopsin-mediated influence
644 on cone signalling is therefore most likely in the retina and involves the intra-retinal retrograde
645 networks from melanopsin cells to outer retina via dopaminergic amacrine cells (Zhang et al.,
646 2008).

647 In conclusion, melanopsin exhibits photic bleaching, although to a lesser extent than
648 cones, with slower regeneration. Our parametrisation of the half-bleaching level and
649 regeneration time-constant for melanopsin phototransduction has implications for estimating
650 the melanopsin bleach level for any light units. Continuous adaptation to lights with higher
651 melanopsin excitation levels but the same photometric luminance results in smaller pupil
652 diameters to improve visual contrast sensitivity.

653

658

659 **Appendix A. Supplementary material**

660 Supplementary data associated with this article can be found, in the online version, at
661 ……………………….

662 **References**

663 Adhikari, P., Zele, A. J., et al. (2019). The melanopsin-directed white noise electroretinogram (wnERG). *Vision*
664 *Research, 164*, 83-93. doi:10.1016/j.visres.2019.08.007

665 Adhikari, P., Zele, A. J., et al. (2015). The post-illumination pupil response (PIPR). *Investigative Ophthalmology*
666 *and Visual Science, 56*(6), 3838-3849. doi:10.1167/iovs.14-16233

667 al Enezi, J., Revell, V., et al. (2011). A "melanopic" spectral efficiency function predicts the sensitivity of
668 melanopsin photoreceptors to polychromatic lights. *Journal of Biological Rhythms, 26*(4), 314-323.
669 doi:10.1177/0748730411409719

670 Allen, A. E., Martial, F. P., et al. (2019). Form vision from melanopsin in humans. *Nature Communications, 10*(1),
671 2274. doi:10.1038/s41467-019-10113-3

672 Allen, A. E., Storchi, R., et al. (2014). Melanopsin-driven light adaptation in mouse vision. *Current Biology,*
673 *24*(21), 2481-2490. doi:10.1016/j.cub.2014.09.015

674 Alpern, M. (1971). Rhodopsin kinetics in the human eye. *The Journal of Physiology, 217*(2), 447-471.
675 doi:10.1113/jphysiol.1971.sp009580

676 Alpern, M., & Campbell, F. (1963). The behaviour of the pupil during dark-adaptation. *Journal of Physiology-*
677 *London, 165*(1), 5-7.

678 Alpern, M., Kitai, S., et al. (1959). The dark-adaptation process of the pupillomotor photoreceptors. *American*
679 *Journal of Ophthalmology, 48(5)*, 583-593. doi:10.1016/0002-9394(59)90609-9

680 Alpern, M., & Ohba, N. (1972). The effect of bleaching and backgrounds on pupil size. *Vision Research, 12*(5),
681 943-951. doi:10.1016/0042-6989(72)90016-8

682 Barlow, H. B. (1972). Dark and light adaptation: psychophysics. In *Visual Psychophysics* (pp. 1-28): Springer.

683 Belenky, M. A., Smeraski, C. A., et al. (2003). Melanopsin retinal ganglion cells receive bipolar and amacrine
684 cell synapses. *Journal of Comparative Neurology, 460*(3), 380-393. doi:10.1002/cne.10652

685 Berson, D. M., Dunn, F. A., et al. (2002). Phototransduction by retinal ganglion cells that set the circadian clock.
686 *Science, 295*(5557), 1070-1073.

687 Boff, K. R., Kaufman, L., et al. (1986). *Handbook of perception and human performance*. New York: Wiley.

688 Brown, T. M., Tsujimura, S., et al. (2012). Melanopsin-based brightness discrimination in mice and humans.
689 *Current Biology, 22*(12), 1134-1141. doi:10.1016/j.cub.2012.04.039

690 Burke, D. W., & Ogle, K. N. (1964). Comparison of Visual and Pupillary Light Thresholds in Periphery. *Archives*
691 *of Ophthalmology, 71(3)*, 400-408. doi:10.1001/archopht.1964.00970010416019

692 Burns, S. A., & Elsner, A. E. (1985). Color matching at high illuminances: the color-match-area effect and
693 photopigment bleaching. *Journal of the Optical Society of America A, 2*(5), 698-704.
694 doi:10.1364/josaa.2.000698

695 Cao, D., & Lu, Y. H. (2012). Lateral suppression of mesopic rod and cone flicker detection. *Journal of the Optical*
696 *Society of America A, 29*(2), A188-193. doi:10.1364/JOSAA.29.00A188

697 Cao, D., Nicandro, N., et al. (2015). A five-primary photostimulator suitable for studying intrinsically
698 photosensitive retinal ganglion cell functions in humans. *Journal of Vision, 15*(1), 15 11 27.
699 doi:10.1167/15.1.27

700 Cao, D., Pokorny, J., et al. (2005). Matching rod percepts with cone stimuli. *Vision Research, 45*(16), 2119-2128.
701 doi:10.1016/j.visres.2005.01.034

702 Cao, D., Pokorny, J., et al. (2008a). Rod contributions to color perception: linear with rod contrast. *Vision*
703 *Research, 48*(26), 2586-2592. doi:10.1016/j.visres.2008.05.001

704 Cao, D., Zele, A. J., et al. (2008b). Chromatic discrimination in the presence of incremental and decremental rod
705 pedestals. *Visual Neuroscience, 25*(3), 399-404. doi:10.1017/S0952523808080425

706 Coile, D. C., & Baker, H. D. (1992). Foveal dark adaptation, photopigment regeneration, and aging. *Visual*
707 *Neuroscience, 8*(1), 27-39. doi:10.1017/s0952523800006465

708 Conner, J. D. (1982). The temporal properties of rod vision. *The Journal of Physiology, 332*, 139-155.
709   doi:10.1113/jphysiol.1982.sp014406

710 Conner, J. D., & MacLeod, D. I. (1977). Rod photoreceptors detect rapid flicker. *Science, 195*(4279), 698-699.
711   doi:10.1126/science.841308

712 Dacey, D. M., Liao, H. W., et al. (2005). Melanopsin-expressing ganglion cells in primate retina signal colour and
713   irradiance and project to the LGN. *Nature, 433*(7027), 749-754. doi:10.1038/nature03387

714 Dartnall, H. J., Bowmaker, J. K., et al. (1983). Human visual pigments: microspectrophotometric results from the
715   eyes of seven persons. *Proceedings of the Royal Society B, 220*(1218), 115-130.
716   doi:10.1098/rspb.1983.0091

717 Dartnall, H. J. A. (1962). Extraction, measurement, and analysis of visual photopigment. *In H. Davson (ed.), The
718   Eye (Vol. 2. pp. 323-365). Academic Press New York:*.

719 DeLawyer, T., Tsujimura, S. I., et al. (2020). Relative contributions of melanopsin to brightness discrimination
720   when hue and luminance also vary. *Journal of the Optical Society of America A, 37*(4), A81-A88.
721   doi:10.1364/JOSAA.382349

722 Do, M. T., Kang, S. H., et al. (2009). Photon capture and signalling by melanopsin retinal ganglion cells. *Nature,
723   457*(7227), 281-287. doi:10.1038/nature07682

724 Emanuel, A. J., & Do, M. T. (2015). Melanopsin tristability for sustained and broadband phototransduction.
725   *Neuron, 85*(5), 1043-1055. doi:10.1016/j.neuron.2015.02.011

726 Feigl, B., Mattes, D., et al. (2011). Intrinsically photosensitive (melanopsin) retinal ganglion cell function in
727   glaucoma. *Investigative Ophthalmology and Visual Science, 52*(7), 4362-4367. doi:10.1167/iovs.10-
728   7069

729 Gamlin, P. D., McDougal, D. H., et al. (2007). Human and macaque pupil responses driven by melanopsin-
730   containing retinal ganglion cells. *Vision Research, 47*(7), 946-954. doi:10.1016/j.visres.2006.12.015

731 Gooley, J. J., Ho Mien, I., et al. (2012). Melanopsin and rod-cone photoreceptors play different roles in mediating
732   pupillary light responses during exposure to continuous light in humans. *Journal of Neuroscience,
733   32*(41), 14242-14253. doi:10.1523/JNEUROSCI.1321-12.2012

734 Güler, A. D., Ecker, J. L., et al. (2008). Melanopsin cells are the principal conduits for rod-cone input to non-
735   image-forming vision. *Nature, 453*(7191), 102-105. doi:10.1038/nature06829

736 Hathibelagal, A. R., Feigl, B., et al. (2016). Correlated and uncorrelated invisible temporal white noise alters
737   mesopic rod signaling. *Journal of the Optical Society of America A, 33*(3), A93-103.
738   doi:10.1364/JOSAA.33.000A93

739 Hecht, S., Haig, C., et al. (1937). The Influence of light adaptation on subsequent dark adaptation of the eye. *The
740   Journal of General Physiology, 20*(6), 831-850. doi:10.1085/jgp.20.6.831

741 Hillman, P., Hochstein, S., et al. (1983). Transduction in invertebrate photoreceptors: role of pigment bistability.
742   *Physiological Review, 63*(2), 668-772. doi:10.1152/physrev.1983.63.2.668

743 Hollins, M., & Alpern, M. (1973). Dark adaptation and visual pigment regeneration in human cones. *The Journal
744   of General Physiology, 62*(4), 430-447. doi:10.1085/jgp.62.4.430

745 Hood, D., & Finkelstein, M. (1986). Sensitivity to light. *Handbook of perception and human performance, (Vol.
746   1: Sensory Processes and Perception)*(Wiley Interscience New York), pp. 5.1-5.66.

747 Hood, D. C. (1998). Lower-level visual processing and models of light adaptation. *Annual Review of Psychology,
748   49(1)*, 503-535. doi:10.1146/annurev.psych.49.1.503

749 Horiguchi, H., Winawer, J., et al. (2013). Human trichromacy revisited. *Proceedings of the National Academy of
750   Sciences, 110*(3), E260-269. doi:10.1073/pnas.1214240110

751 Jacobs, G. H., & Williams, G. A. (2007). Contributions of the mouse UV photopigment to the ERG and to vision.
752   *Documenta Ophthalmologica, 115*(3), 137-144. doi:10.1007/s10633-007-9055-z

753 Joselevitch, C. (2008). Human retinal circuitry and physiology. *Psychology & Neuroscience, 1*(2), 141-165.
754   doi:10.3922/j.psns.2008.2.008

755 Kardon, R., Anderson, S. C., et al. (2009). Chromatic pupil responses: preferential activation of the melanopsin-
756 mediated versus outer photoreceptor-mediated pupil light reflex. *Ophthalmology, 116*(8), 1564-1573.
757 doi:10.1016/j.ophtha.2009.02.007

758 Kelbsch, C., Strasser, T., et al. (2019). Standards in pupillography. *Frontiers in Neurology, 10*, 129.
759 doi:10.3389/fneur.2019.00129

760 Kolb, H., Fernandez, E., et al. (1995). Photoreceptors--webvision: the organization of the retina and visual system.

761 Lamb, T. D. (1981). The involvement of rod photoreceptors in dark adaptation. *Vision Research, 21*(12), 1773-
762 1782. doi:10.1016/0042-6989(81)90211-x

763 Lamb, T. D., & Pugh, E. N., Jr. (2004). Dark adaptation and the retinoid cycle of vision. *Progress in Retinal and
764 Eye Research, 23*(3), 307-380. doi:10.1016/j.preteyeres.2004.03.001

765 Loewenfeld, I. E., & Lowenstein, O. (1993). *The Pupil: Anatomy, Physiology, and Clinical Applications (Vol. 1).*
766 *Boston: Butterworth-Heinemann.*

767 Lyubarsky, A. L., Daniele, L. L., et al. (2004). From candelas to photoisomerizations in the mouse eye by
768 rhodopsin bleaching in situ and the light-rearing dependence of the major components of the mouse ERG.
769 *Vision Research, 44*(28), 3235-3251. doi:10.1016/j.visres.2004.09.019

770 MacLeod, D. I. (1978). Visual sensitivity. *Annual Review of Psychology, 29*, 613-645.
771 doi:10.1146/annurev.ps.29.020178.003145

772 Mahroo, O. A., & Lamb, T. D. (2004). Recovery of the human photopic electroretinogram after bleaching
773 exposures: estimation of pigment regeneration kinetics. *The Journal of Physiology, 554*(2), 417-437.
774 doi:10.1113/jphysiol.2003.051250

775 Mahroo, O. A., & Lamb, T. D. (2012). Slowed recovery of human photopic ERG a-wave amplitude following
776 intense bleaches: a slowing of cone pigment regeneration? *Documenta Ophthalmologica, 125*(2), 137-
777 147. doi:10.1007/s10633-012-9344-z

778 Markwell, E. L., Feigl, B., et al. (2010). Intrinsically photosensitive melanopsin retinal ganglion cell contributions
779 to the pupillary light reflex and circadian rhythm. *Clinical and Experimental Optometry, 93*(3), 137-149.
780 doi:10.1111/j.1444-0938.2010.00479.x

781 McDougal, D. H., & Gamlin, P. D. (2010). The influence of intrinsically-photosensitive retinal ganglion cells on
782 the spectral sensitivity and response dynamics of the human pupillary light reflex. *Vision Research,
783 50*(1), 72-87. doi:10.1016/j.visres.2009.10.012

784 Mure, L. S., Cornut, P. L., et al. (2009). Melanopsin bistability: a fly's eye technology in the human retina. *PLoS
785 One, 4*(6), e5991. doi:10.1371/journal.pone.0005991

786 Naarendorp, F., Esdaille, T. M., et al. (2010). Dark light, rod saturation, and the absolute and incremental
787 sensitivity of mouse cone vision. *Journal of Neuroscience, 30*(37), 12495-12507.
788 doi:10.1523/JNEUROSCI.2186-10.2010

789 Nikonov, S. S., Daniele, L. L., et al. (2005). Photoreceptors of Nrl -/- mice coexpress functional S- and M-cone
790 opsins having distinct inactivation mechanisms. *The Journal of General Physiology, 125*(3), 287-304.
791 doi:10.1085/jgp.200409208

792 Nikonov, S. S., Kholodenko, R., et al. (2006). Physiological features of the S- and M-cone photoreceptors of wild-
793 type mice from single-cell recordings. *The Journal of General Physiology, 127*(4), 359-374.
794 doi:10.1085/jgp.200609490

795 Ohba, N., & Alpern, M. (1972). Adaptation of the pupil light reflex. *Vision Research, 12*(5), 953-967.
796 doi:10.1016/0042-6989(72)90017-X

797 Ostrin, L. A., Strang, C. E., et al. (2018). Immunotoxin-induced ablation of the intrinsically photosensitive retinal
798 ganglion cells in rhesus monkeys. *Frontiers in Neurology, 9*, 1000. doi:10.3389/fneur.2018.01000

799 Paupoo, A. A., Mahroo, O. A., et al. (2000). Human cone photoreceptor responses measured by the
800 electroretinogram a-wave during and after exposure to intense illumination. *The Journal of Physiology,
801 529*(2), 469-482. doi:10.1111/j.1469-7793.2000.00469.x

802 Pianta, M. J., & Kalloniatis, M. (2000). Characterisation of dark adaptation in human cone pathways: an
803 application of the equivalent background hypothesis. *The Journal of Physiology, 528*(Pt 3), 591-608.
804 doi:10.1111/j.1469-7793.2000.00591.x

805 Pokorny, J., Smithson, H., et al. (2004). Photostimulator allowing independent control of rods and the three cone
806   types. *Visual Neuroscience, 21*(3), 263-267. doi:10.1017/S0952523804213207

807 Prigge, C. L., Yeh, P. T., et al. (2016). M1 ipRGCs influence visual function through retrograde signaling in the
808   retina. *Journal of Neuroscience, 36*(27), 7184-7197. doi:10.1523/JNEUROSCI.3500-15.2016

809 Provencio, I., Rodriguez, I. R., et al. (2000). A novel human opsin in the inner retina. *Journal of Neuroscience,*
810   *20*(2), 600-605. doi:10.1523/JNEUROSCI.20-02-00600.2000

811 Pugh, E. N. (1975). Rushton's paradox: rod dark adaptation after flash photolysis. *The Journal of Physiology,*
812   *248*(2), 413-431. doi:10.1113/jphysiol.1975.sp010982

813 Rebec, K. M., & Gunde, M. K. (2014). High-performance lighting evaluated by photobiological parameters.
814   *Applied Optics, 53*(23), 5147-5153. doi:10.1364/AO.53.005147

815 Reuter, T. (2011). Fifty years of dark adaptation 1961-2011. *Vision Research, 51*(21-22), 2243-2262.
816   doi:10.1016/j.visres.2011.08.021

817 Revell, V. L., & Skene, D. J. (2007). Light-induced melatonin suppression in humans with polychromatic and
818   monochromatic light. *Chronobiology International, 24*(6), 1125-1137.
819   doi:10.1080/07420520701800652

820 Ripps, H., & Weale, R. A. (1969). Flash bleaching of rhodopsin in the human retina. *The Journal of Physiology,*
821   *200*(1), 151-159. doi:10.1113/jphysiol.1969.sp008686

822 Rushton, W. A. (1961). Dark-adaptation and the regeneration of rhodopsin. *The Journal of Physiology, 156*, 166-
823   178. doi:10.1113/jphysiol.1961.sp006666

824 Rushton, W. A., & Henry, G. H. (1968). Bleaching and regeneration of cone pigments in man. *Vision Research,*
825   *8*(6), 617-631. doi:10.1016/0042-6989(68)90040-0

826 Schmidt, T. M., Alam, N. M., et al. (2014). A role for melanopsin in alpha retinal ganglion cells and contrast
827   detection. *Neuron, 82*(4), 781-788. doi:10.1016/j.neuron.2014.03.022

828 Sekaran, S., Foster, R. G., et al. (2003). Calcium imaging reveals a network of intrinsically light-sensitive inner-
829   retinal neurons. *Current Biology, 13*(15), 1290-1298. doi:10.1016/s0960-9822(03)00510-4

830 Sexton, T. J., Golczak, M., et al. (2012). Melanopsin is highly resistant to light and chemical bleaching in vivo.
831   *Journal of Biological Chemistry, 287*(25), 20888-20897. doi:10.1074/jbc.M111.325969

832 Smith, V. C., & Pokorny, J. (1975). Spectral sensitivity of the foveal cone photopigments between 400 and 500
833   nm. *Vision Research, 15*(2), 161-171. doi:10.1016/0042-6989(75)90203-5

834 Smith, V. C., Pokorny, J., et al. (1983). Densitometric measurement of human cone photopigment kinetics. *Vision*
835   *Research, 23*(5), 517-524. doi:10.1016/0042-6989(83)90126-8

836 Spitschan, M. (2019a). Melanopsin contributions to non-visual and visual function. *Current Opinion in*
837   *Behavioral Sciences, 30*, 67-72. doi:10.1016/j.cobeha.2019.06.004

838 Spitschan, M. (2019b). Photoreceptor inputs to pupil control. *Journal of Vision, 19*(9), 5. doi:10.1167/19.9.5

839 Spitschan, M., Aguirre, G. K., et al. (2015). Selective stimulation of penumbral cones reveals perception in the
840   shadow of retinal blood vessels. *PLoS One, 10*(4), e0124328. doi:10.1371/journal.pone.0124328

841 Spitschan, M., Bock, A. S., et al. (2017). The human visual cortex response to melanopsin-directed stimulation is
842   accompanied by a distinct perceptual experience. *Proceedings of the National Academy of Sciences,*
843   *114*(46), 12291-12296. doi:10.1073/pnas.1711522114

844 Sun, H., Pokorny, J., et al. (2001). Control of the modulation of human photoreceptors. *Color Research and*
845   *Application, 26 (S1)*. doi:10.1002/1520-6378(2001)26:1+<::AID-COL16>3.0.CO;2-A

846 Teikari, P., Najjar, R. P., et al. (2012). Refined flicker photometry technique to measure ocular lens density.
847   *Journal of the Optical Society of America A, 29*(11), 2469-2478. doi:10.1364/JOSAA.29.002469

848 Thomas, M. M., & Lamb, T. D. (1999). Light adaptation and dark adaptation of human rod photoreceptors
849   measured from the a-wave of the electroretinogram. *The Journal of Physiology, 518*(2), 479-496.
850   doi:10.1111/j.1469-7793.1999.0479p.x

851 Tsujimura, S., Ukai, K., et al. (2010). Contribution of human melanopsin retinal ganglion cells to steady-state
852   pupil responses. *Proceedings of the Royal Society B, 277*(1693), 2485-2492. doi:10.1098/rspb.2010.0330

853 Tu, D. C., Owens, L. A., et al. (2006). Inner retinal photoreception independent of the visual retinoid cycle.
854   *Proceedings of the National Academy of Sciences, 103*(27), 10426-10431. doi:10.1073/pnas.0600917103

855 Wald, G., Durell, J., et al. (1950). The light reaction in the bleaching of rhodopsin. *Science, 111*(2877), 179-181.
856   doi:10.1126/science.111.2877.179

857 Wong, K. Y. (2012). A retinal ganglion cell that can signal irradiance continuously for 10 hours. *Journal of
858   Neuroscience, 32*(33), 11478-11485. doi:10.1523/JNEUROSCI.1423-12.2012

859 Wyszecki, G., & Stiles, W. S. (1982). *Color Science (2nd ed.)* (Vol. 8): New York: Wiley.

860 Zele, A. J., Adhikari, P., et al. (2019a). Melanopsin and cone photoreceptor inputs to the afferent pupil light
861   response. *Frontiers in Neurology, 10*, 529.

862 Zele, A. J., Adhikari, P., et al. (2019b). Melanopsin driven enhancement of cone-mediated visual processing.
863   *Vision Research, 160*, 72-81. doi:10.1016/j.visres.2019.04.009

864 Zele, A. J., & Cao, D. (2015). Vision under mesopic and scotopic illumination. *Frontiers in Psychology, 5*, 1594.
865   doi:10.3389/fpsyg.2014.01594

866 Zele, A. J., Dey, A., et al. (2020a). Melanopsin hypersensitivity dominates interictal photophobia in migraine.
867   *Cephalalgia*, 333102420963850. doi:10.1177/0333102420963850

868 Zele, A. J., Dey, A., et al. (2020b). Rhodopsin and melanopsin contributions to human brightness estimation.
869   *Journal of the Optical Society of America A, 37*(4), A145-A153. doi:10.1364/JOSAA.379182

870 Zele, A. J., Feigl, B., et al. (2018). Melanopsin photoreception contributes to human visual detection, temporal
871   and colour processing. *Sci Rep, 8*(1), 3842. doi:10.1038/s41598-018-22197-w

872 Zele, A. J., Feigl, B., et al. (2011). The circadian response of intrinsically photosensitive retinal ganglion cells.
873   *PLoS One, 6*(3), e17860. doi:10.1371/journal.pone.0017860

874 Zele, A. J., & Gamlin, P. D. (2020). Editorial: The Pupil: Behavior, Anatomy, Physiology and Clinical
875   Biomarkers. *Frontiers in Neurology, 11*, 211. doi:10.3389/fneur.2020.00211

876 Zhang, D. Q., Wong, K. Y., et al. (2008). Intraretinal signaling by ganglion cell photoreceptors to dopaminergic
877   amacrine neurons. *Proceedings of the National Academy of Sciences, 105*(37), 14181-14186.
878   doi:10.1073/pnas.0803893105

879 Zhao, X., Pack, W., et al. (2016). Prolonged inner retinal photoreception depends on the visual retinoid cycle.
880   *Journal of Neuroscience, 36*(15), 4209-4217. doi:10.1523/JNEUROSCI.2629-14.2016